Yeast
Yeast 2003; **20**: 295–314.
Published online in Wiley InterScience (www.interscience.wiley.com). **DOI:** 10.1002/yea.960

Research Article

Proteome analysis of recombinant xylose-fermenting *Saccharomyces cerevisiae*

Laura Salusjärvi[1]*, Marjo Poutanen[2], Juha-Pekka Pitkänen[1#], Heini Koivistoinen[2], Aristos Aristidou[1##], Nisse Kalkkinen[2], Laura Ruohonen[1] and Merja Penttilä[1]
[1] *VTT Biotechnology, PO Box 1500, FIN-02044 VTT, Finland*
[2] *Institute of Biotechnology, Laboratory of Protein Chemistry, PO Box 56, 00014 University of Helsinki, Finland*

**Correspondence to: Laura Salusjärvi, VTT Biotechnology, PO Box 1500, FIN-02044 VTT, Finland. E-mail: laura.salusjarvi@vtt.fi*

 # Current address: MediCel Ltd, Haartmaninkatu 8, FIN-00290 Helsinki, Finland.

Current address: Cargill Dow LLC, 15305 Minnetonka Boulevard, Minnetonka, MN 55345, USA.

Received: 22 July 2002
Accepted: 11 November 2002

Abstract

Introduction of an active xylose utilization pathway into *Saccharomyces cerevisiae*, which does not naturally ferment pentose sugars, is likely to have a major impact on the overall cellular metabolism as the carbon introduced to the cells will now flow through the pentose phosphate pathway. The metabolic responses in the recombinant xylose-fermenting *S. cerevisiae* were studied at the proteome level by comparative two-dimensional gel electrophoresis of cellular proteins within a pH range of 3–10. Glucose-limited chemostat cultivations and corresponding chemostat cultivations performed in media containing xylose as the major carbon source were compared. The cultivations were studied in aerobic and anaerobic metabolic steady states and in addition at time points 5, 30 and 60 min after the switch-off of oxygen supply. We identified 22 proteins having a significant abundance difference on xylose compared to glucose, and 12 proteins that responded to change from aerobic to anaerobic conditions on both carbon sources. On xylose in all conditions studied, major changes were seen in the abundance of alcohol dehydrogenase 2 (Adh2p), acetaldehyde dehydrogenases 4 and 6 (Ald4p and Ald6p), and DL-glycerol 3-phosphatase (Gpp1p). Our results give indications of altered metabolic fluxes especially in the acetate and glycerol pathways in cells growing on xylose compared to glucose. Copyright © 2003 John Wiley & Sons, Ltd.

Keywords: ***Saccharomyces cerevisiae*; xylose; ethanol; proteome; proteomics; two-dimensional gel electrophoresis; pentose phosphate pathway; metabolic engineering**

Introduction

Although *Saccharomyces cerevisiae* is not able to ferment or grow on xylose, it has been reported to metabolize it at a slow rate (van Zyl *et al*., 1989) and evidence for endogenous genes encoding all three xylose pathway enzymes; xylose reductase, xylitol dehydrogenase and xylulokinase exists (Batt *et al*., 1986; Ho and Chang, 1989; Kuhn *et al*., 1995; Richard *et al*., 1999, 2000). Our laboratory has constructed a xylose-utilizing yeast strain by introducing the genes encoding xylose reductase (*XYL1*; XR) and xylitol dehydrogenase (*XYL2*; XDH) from the yeast *Pichia stipitis* (Kötter *et al*., 1990) into *S. cerevisiae* and recently by over-expressing the endogenous xylulokinase encoding gene (*XKS1*; XK) (Richard *et al*., 2000; Toivari *et al*., 2001). These enzymes catalyse the sequential reduction of xylose to xylitol (XR) and oxidation of xylitol to xylulose (XDH), followed by the phosphorylation of xylulose to xylulose-5-phosphate (XK), which can then enter the pentose phosphate pathway and subsequently be converted to ethanol. As a result, aerobic growth and even anaerobic ethanol production on xylose have been achieved, but still a large fraction of consumed xylose is excreted as xylitol (Eliasson *et al*., 2000; Ho *et al*., 1998; Toivari *et al*., 2001).

The introduction of these two redox enzymes is expected to have a major impact on the redox balance of the cell. This has been suggested to be one of the major reasons for inefficient incorporation of xylose-derived carbon into the central pathways leading to ethanol (Kötter and Ciriacy, 1993). Xylose reductase has a preference for NADPH over NADH, while xylitol dehydrogenase is specific for NAD^+. Consequently, the conversion of xylose to xylulose results in net NADPH consumption and NADH formation, even though the conversion is overall redox neutral. Especially under anaerobic conditions, this leads to production of unwanted side products such as xylitol (Kötter and Ciriacy, 1993).

S. cerevisiae is assumed to import xylose via the same system as glucose and the possibility that uptake of xylose is a significant limiting step in xylose fermentation cannot be excluded. The reactions downstream of XDH, including the step converting xylulose to xylulose-5-phosphate as well as subsequent transketolase and transaldolase reactions, may also be limiting. In a strain without overexpressed xylulokinase, overexpression of the transaldolase-encoding gene enhanced growth on xylose, but not in a strain overexpressing xylulokinase (Johansson and Hahn-Hägerdal, 2002; Walfridsson *et al*., 1995). However, overexpression of the endogenous xylulokinase-encoding gene was shown to have a more profound effects with decreased secretion of xylitol, increased flux to ethanol and increased ethanol yield on xylose in aerobic and anaerobic conditions (Eliasson *et al*., 2000; Toivari *et al*., 2001). In spite of this, metabolic rates and ethanol yields obtained on this pentose sugar remain still considerably below the levels achieved when hexose sugars are employed.

For the analysis of the overall protein pattern and abundancies proteomics methods offer an attractive and global strategy, and can be used to study the effects of the introduction of the xylose pathway on the cellular metabolism of *S. cerevisiae*. Proteome analysis is already well established in yeast but there are nevertheless relatively few examples of its effective application in order to understand and solve real metabolic problems, although the number of studies is constantly increasing (Brejning and Jespersen, 2002; Godon *et al*., 1998; Gygi *et al*., 1999a; Haurie *et al*., 2001; Norbeck and Blomberg, 1997; Vido *et al*., 2001). However, yeast has been widely used as a model organism for the methodological development of analytical techniques of protein profiling (large-scale protein identification), for characterization of protein complexes and for studies of protein–protein interactions. The latter two are becoming increasingly popular and, combined with biological and genomic data, the information of protein–protein interactions helps to provide a physical map of the cell (Blackstock and Mann, 1999; Gavin *et al*., 2002; Gottschalk *et al*., 1999; Ho *et al*., 2002; Shevchenko *et al*., 1996; Uetz *et al*., 2000).

In our study, we carried out controlled chemostat cultures where the cell physiology can be kept in a steady state. We used xylose or glucose as carbon sources and both aerobic and anaerobic conditions. In addition, we studied the short-term response of the proteome to oxygen depletion. Protein spots displaying variation in intensities between different cultivations were identified by mass spectrometry. Our results indicate how the yeast responds to the redox co-factor imbalance created in the xylose pathway and offer also new insights, for the first time at the proteome level, to the metabolism of xylose in recombinant *S. cerevisiae*. Major differences observed in cells on xylose compared to glucose centralize around the redox-balancing reactions.

Materials and methods

Yeast strain

The genetically modified *Saccharomyces cerevisiae* strain H2490, constructed from the parent strain CEN.PK2 (*MATα,leu2*-3/112, *ura3-52, trp1-289, his3*Δ *1,MAL2-8*^{c}, *SUC*2) (Boles *et al*., 1996) was used for all experiments. The strain H2490 contains the *XYL1* and *XYL2* genes of *Pichia stipitis*, encoding xylose reductase and xylitol dehydrogenase, respectively, chromosomally integrated into the *URA3* locus. *XYL1* is expressed under the constitutive *PGK1* promoter and *XYL2* under the modified *ADH1* promoter (Ruohonen *et al*., 1995). In addition, the strain contains the endogenous xylulokinase-encoding gene from *S. cerevisiae* between the modified *ADH1* promoter and terminator on a multicopy plasmid YEplac195 (uracil selection) and the multicopy plasmid YEplac181 (leucine selection) (Gietz and Sugino, 1988) with

the *PGK1* promoter and terminator expression cassette with no insert. The *PGK1* promoter and terminator were isolated by *Hin*dIII digestion as an 1800 bp fragment from pMA91 (Mellor *et al*., 1983).

H2490 is also cured for its histidine and tryptophan auxotrophies by integrating *HIS3* and *TRP1* genes back to their respective loci. For the integration, a 1500 bp fragment containing the *HIS3* gene was isolated from plasmid pRS423 (Christianson *et al*., 1992) and a 1300 bp fragment of *TRP1* from pRS424 (Christianson *et al*., 1992) by *Drd*I digestion. The strain H2490 was transformed with the above-mentioned fragments separately by the lithium acetate transformation method and plated on synthetic complete plates containing 2% glucose but without histidine or tryptophan, respectively, for *HIS3* integration selection or *TRP1* integration selection. The *Drd*I fragment used in both cases had, in addition to the functional *HIS3* or *TRP1*, some vector sequence at both 5′ and 3′ ends. The correct integration was confirmed by amplifying the *HIS3* or *TRP1* region outside of the recombination site and sequencing the PCR fragment at 3′ and 5′ ends to make sure that no vector sequence had integrated into the yeast chromosome.

Chemostat cultivations

The yeast precultures were grown in 50 ml of yeast nitrogen base (YNB, Sigma) supplemented with 20 g/l glucose in 250 ml shake flasks for 20 h at 30 °C with agitation of 200 rpm. Cells were harvested by centrifugation and resuspended in 50 ml of cultivation media aiming at a starting optical density (OD_{600}) in the fermenter cultivation of about 1.

The chemostat cultivations were carried out with a working volume of 800 ml in 1.8 l Chemap CMF fermenters (Chemap AG, Switzerland) fed with YNB without amino acids, supplemented with 0.5 ml/l silicone antifoam (AnalaR, BDH) and either 10 g/l glucose, or 27 g/l xylose and 3 g/l glucose. The cultivations were performed at 30 °C, with an agitation speed of 500 rpm and a pH of 5.5 maintained with 1 M KOH and 1 M H_3PO_4. The total gas flow under both aerobic and anaerobic conditions was 0.4 L/min maintained by two mass flow controllers (Bronkhorst High-Tech BV, The Netherlands). Anaerobic conditions were achieved by sparging the bioreactor with nitrogen (99.999% AGA quality 5.0, Finland).

Both fermentations were started as aerobic batch cultures run until the carbon dioxide level was stabilized. The feed flow of the medium was started at this point yielding a dilution rate (D) of 0.05/h. Both cultivations were glucose-limited but the cultures carried out aerobically and anaerobically on 10 g/l glucose had higher volumetric biomass content than the xylose-grown cultures (Table 1). Cultivation conditions were maintained

Table 1. Carbon uptake rates and productivities under steady-state conditions. Specific (C-mmol/g-cell/h) (A) and volumetric rates (C-mmol/h/l) (B) of glucose, xylose and oxygen (OUR) consumption and formation of carbon dioxide (CER), biomass, xylitol, glycerol, acetate and ethanol in the continuous cultivation of the strain H2490 on 27 g/l xylose with 3 g/l glucose (XYL27/GLC3) and on 10 g/l glucose (GLC10) under aerobic (after 7.5 residence times) and anaerobic (after 6.6 residence times) conditions

	Glucose	Xylose	OUR	CER	Biomass	Xylitol	Glycerol	Acetate	Ethanol
(A) Unit: C-mmol/g-cell/h									
Aerobic									
GLC10	−7.22	0	−4.19	4.26	1.86	0	<0.01	0.81	0.48
XYL27/GLC	−1.95	−3.62	−2.26	2.76	1.93	0.74	0.06	0.02	0.04
Anaerobic									
GLC10	−27.2	0	0	8.60	1.85	0	2.88	0.66	10.6
XYL27/GLC	−19.1	−15.4	0	7.49	1.83	7.62	2.78	1.04	12.6
(B) Unit: C-mmol/h/l									
Aerobic									
GLC 10	−17.66	0	−10.25	10.43	4.56	0	0	1.98	1.18
XYL/GLC 3	−4.86	−9.02	−5.63	6.88	4.81	1.85	0.15	0.06	0.10
Anaerobic									
GLC 10	−16.02	0	0	5.07	1.09	0	1.70	0.39	6.24
XYL/GLC 3	−4.36	−3.50	0	1.71	0.42	1.74	0.63	0.24	2.88

for 6.5 residence times (time required for replacing 6.5 times the reactor content) under aerobic conditions to obtain a metabolic steady state. For fractional NMR studies performed from these same cultivations (Maaheimo *et al.*, manuscript in preparation), media containing U-^{13}C-glucose (Martek Biosciences Corporation, USA) were applied for one residence time at this point. The total amount of labelled glucose used was 0.1% for both cultivation media used. After two residence times from the end of the feed of the labelled media the chemostats were changed from aerobic to the anaerobic cultivation. Feed of the non-labelled media was continued for 5.4 residence times before the feed of labelled media was again started for one residence time.

For proteomics studies, 10–20 ml culture samples were taken from the labelled phases of the aerobic and anaerobic steady states and from time points of 5, 30 and 60 min after the switch-off of oxygen supply. Cells were harvested by centrifugation (3500 rpm, 2 min at 20 °C), washed once with 0.9% NaCl and after that immediately frozen by liquid nitrogen and stored at −70 °C.

Growth and extracellular products

Cell density was followed optically (Shimadzu, Japan) at 600 nm (OD_{600}) or gravimetrically by measuring the cell dry weight. For cell dry weight (CDW, g/l) a known volume of culture sample was centrifuged (4000 rpm/3000 × *g*, 5 min at +4 °C) and washed with distilled water. The precipitate was dried overnight at +105 °C on pre-weighed dry weight cups and then weighted. The extracellular metabolite samples were obtained by filtering the supernatant through a 0.45 μm syringe filter (MILLEX-GS, Millipore, France) and stored at −20 °C. Glucose, xylose, xylitol, glycerol, acetate and ethanol were measured from filtered cultivation samples with a Waters HPLC system. The system consisted of a 510 pump, 717 autosampler, column oven, Aminex HPX-87H column (Bio-Rad, USA) at 35 °C, 410 refractive index (RI) detector and 2487 dual λ UV detector.

The fermenter outlet gas composition was analysed on-line using a QMG 421C quadrupole mass spectrometer (Balzers Pfeiffer Scandinavia AB, Sweden). The Balzers Quadstar 422 software was employed to calculate the percentage mole fractions of O_2, CO_2, N_2 and Ar. The system was calibrated using two gases containing $Ar/O_2/N_2$ at 20 : 20 : 60 vol% and CO_2 : Ar at 3 : 97 vol% (Messer Griesheim, Germany).

Preparation of protein extract for isoelectric focusing

5–10 mg dry mass of cells was resuspended in 150 μl 50 mM Hepes, pH 7, 1 mM $MgCl_2$, 0.1 mM EDTA supplemented with phenylmethylsulphonyl fluoride (Sigma, USA) to 1 mM and Pepstatin A (Sigma) to a concentration of 13 μM. 100 μl glass beads (0.5 mm diameter; Biospec Products, USA) were added to the cell suspension and the suspension in 1.5 ml microcentrifuge tubes was inserted into a MiniBeadbeater 8 (Biospec Products) and shaken at homogenization speed four times for 30 s. The tubes were cooled on ice between each homogenization step. After cell breakage, 400 μl lysis buffer consisting of 7 M urea (Promega, USA), 2 M thiourea (Fluka, USA), 4% CHAPS (Fluka), 1% Pharmalytes 3–10 (Pharmacia, Sweden) and 1% DTT (Sigma) was added into the tubes and the mixture was incubated by gently shaking for 20 min at room temperature. The supernatants were then withdrawn and centrifuged for 5 min at 13 000 rpm. The protein concentration of supernatants was determined by the non-interfering protein assay (Gene Technology Inc., USA) and the samples were stored at −70 °C before isoelectric focusing.

Two-dimensional polyacrylamide gel electrophoresis

The first dimension of the two-dimensional polyacrylamide gel electrophoresis (2D-PAGE) was performed on an IPGphor™ (Amersham Pharmacia Biotech AB, Sweden) isoelectric focusing apparatus. Non-linear, 18 cm long, pH 3–10 Immobiline gels (IPG-strips; Amersham Pharmacia Biotech AB) were rehydrated in a strip holder for 6 h in 350 μl rehydration buffer containing 9 M urea (Promega), 0.5% CHAPS (Fluka), 0.2% DTT (Sigma), 0.5% Pharmalytes 3–10 (Pharmacia) and 75 μg protein extract. Isoelectric focusing was carried out at 20 °C with the following settings: 30 V, 6 h; 150 V, 1 h; 300 V, 1 h; 600 V, 1 h; linear gradient 600–5000 V, 4 h; and 5000 V, 12 h or until 70 000 Vh was reached. Prior to the second dimension, the IPG-strips were equilibrated for 10 min in 30 ml of 50 mM Tris–HCl, pH 8.8, 6 M urea

(Promega), 30% glycerol, 2% SDS and 1% (w/v) DTT (Sigma) and then a further 10 min in the same buffer in which DTT was replaced with 4.5% (w/v) iodoacetamide (Sigma).

The second dimension, 12% SDS–PAGE (Laemmli, 1970), was carried out in a Hoefer DALT electrophoresis tank (Pharmacia). After the electrophoresis, the gels were fixed for 1.5 h in 30% ethanol and 0.5% acetic acid and silver-stained using the method of O'Connell and Stults (1997).

Scanning and computerized data analysis

Silver-stained 2D gels were scanned using a GS-710 Imaging Densitometer (Bio-Rad, USA) and raw scans were processed using the 2D software PDQuest (Bio-Rad). The gel scans were first subjected to background subtraction and smoothing to produce a synthetic gel image. The different gel patterns were then automatically, with some additional manual editing, matched to each other and the quantities of matched spots in different gels were compared. For each sample, mean spot quantities were derived from three or four gels run in parallel. The quantification of proteins resolved was normalized to the total optical density in each gel image. The statistical and quantitative analyses were performed utilizing functions within the PDQuest software. Proteins displaying significant changes in quantity between aerobic and anaerobic steady-state samples taken from two different cultivations were selected using Student's *t*-test.

Protein identification

Proteins were excised from the gel, destained, reduced, alkylated and digested in-gel with trypsin, as described previously (Poutanen *et al*., 2001). After desalting, the tryptic peptides were subjected to matrix-assisted laser desorption/ionization (MALDI) mass spectrometric analysis. MALDI–TOF mass spectra for mass mapping of tryptic peptides were acquired using a Biflex™ matrix-assisted laser desorption time-of-flight instrument (Bruker-Daltonik GmbH, Bremen, Germany), equipped with a nitrogen laser operating at 337 nm in a positive ion reflector mode. α-Cyano-4-hydroxycinnamic acid was used as the matrix. The MALDI mass spectra were internally calibrated with angiotensin II and ACTH-clip 18–39 (Sigma-Aldrich Chemie GmbH). The mass spectrometer parameters were optimized for the measuring range of 900–2500 Da.

In cases where the identity of proteins present was not established by MALDI analysis alone, a nanospray liquid chromatography/electrospray ionization tandem mass spectrometer (LC–MS–MS) was used for sequence tag analysis (Poutanen *et al*., 2001). For these LC–MS–MS analyses, the digests were either desalted and concentrated or loaded into a precolumn (0.3 mm × 1 mm PepMap, MGU-30-C18PM, LCPackings, The Netherlands) at a flow rate of 10 µl/min. After the pre-concentration and clean-up steps, the precolumn was switched in-line with the LC. For LC–MS–MS analysis, reversed phase chromatography was performed on an Ultimate nanochromatography apparatus (LC Packings, The Netherlands), using a 75 µm i.d. ×15 cm PepMap column (NAN75-15-03-C18-PM, LC Packings). In a typical analysis, 1–2 µl desalted sample were injected in LC.

Positive ion electrospray ionization (ESI) spectra were recorded using a Q-TOF hybrid mass spectrometer (Micromass Ltd, Manchester, UK) equipped with an orthogonal electrospray source (Z-spray) and a modified nano ES-interface (LTQ-ADP, New Objective Inc., Cambridge, MA). The HPLC column effluents were delivered directly through a fused silica capillary to the electrospray needle, which was a fused silica distal-end coated tip (FS360-20-10-D-20; New Objective Inc.).

The programs and servers used for protein identification with mass map-data were: ProFound, in **http://prowl.rockefeller.edu/cgi-bin/ProFound;** Peptide map, in **PepSea in http://pepsea.protana.com/**; and MS-Fit, in **http://prospector.ucsf.edu/mshome3.2.htm**. For identification of sequence tag data we used the following programs and servers: Sequence Tag, in **PepSea in http://pepsea.protana.com/;** ProteinInfo, in **http://prowl1.rockefeller.edu/prowl/proteininfo.html;** and MS-Tag, in **http://prospector.ucsf.edu/ucsfhtml3.2/mstagfd.htm**.

Results

Chemostat cultivations and experimental design

Two different types of chemostat cultivations, both with aerobic (20% oxygen) and anaerobic (0%

oxygen) phases, were carried out with the recombinant *S. cerevisiae* strain H2490 harbouring the genes for XR and XDH from *P. stipitis* integrated into the *S. cerevisiae* genome and the endogenous gene for XK on a multicopy plasmid. The first cultivation was carried out with 10 g/l glucose and the second with 3 g/l glucose + 27 g/l xylose. The same dilution rate (D) of 0.05/h was used for all four chemostat conditions studied in order to keep the growth rate constant, and so avoid growth rate-dependent changes in the proteome (Hayes *et al.*, 2002). The small amount of glucose was added in the feed of the latter chemostat to enable anaerobic growth on xylose. Specific and volumetric rates of carbon utilization and metabolite production in aerobic and anaerobic steady states are presented in Table 1 (see also Juha-Pekka Pitkänen *et al.*, in press). Of the four conditions studied, the specific ethanol production rate was highest (12.6 C-mmol/h/g) on the xylose + glucose mixture under anaerobic conditions. Under aerobic conditions, 20% xylose was excreted as xylitol, whereas under anaerobic conditions the corresponding amount was 50%. The residual glucose on both glucose and on 3 g/l glucose + 27 g/l xylose culture was 0 under both aerobic and anaerobic conditions. Thus, the growth modes compared in our study are glucose-limited and can be regarded as growth and metabolism on glucose under glucose-derepressed conditions and growth and metabolism on xylose, since glucose repression should not be present in glucose-limited chemostat cultivations performed under our conditions (Meijer *et al.*, 1998; Sierkstra *et al.*, 1992; ter Linde *et al.*, 1999). Hence, from here onward we simply refer to glucose and xylose cultivations.

Protein extracts from the cells harvested from aerobic and anaerobic steady states of the glucose and xylose chemostats were analysed by comparative 2D gel electrophoresis. An example is shown in Figure 1. Samples from time points 5, 30 and 60 min after the switch-off of oxygen (see Materials and methods) were also analysed. For technical reasons, silver staining was used for spot detection, although it is less sensitive and tends to underestimate variation of more abundant proteins compared, for instance, to radioactive labelling.

Quantification of changes in protein expression

The silver stained gel scans were processed by the image analysis software PDQuest. The total number of spots resolved and quantified in each gel was on average 833 ± 83 (SD: $n = 33$) and there were no significant differences in spot numbers between the gels run from glucose and xylose samples. After spot detection, the gels were matched to each other with the help of the so-called landmark function and, according to PDQuest software, 659 spots in total could be matched in all 33 gels analysed. At this point spots that were near the background in their intensity in all gels were discarded from the analysis. In no case was a dominant or well-focused spot unmatched. The individual protein spots on the gels were quantified and normalized to the total optical density in gel images.

For analysis of changes in the protein patterns, three to four gels were run from each individual sample and mean quantitative values and standard deviations were calculated for each protein spot. The Student's t-test within PdQuest software was performed to find statistically significant changes between aerobic and anaerobic glucose and xylose steady-state samples. According to this test, proteins were divided into groups corresponding to their response either to the carbon source used or to the level of oxygen during the cultivations. Only a few proteins had a clear gradual response to the switch from aerobic to anaerobic conditions within the 1 h transition time studied. Differences were mainly seen between samples taken from the fully aerobic and completely anaerobic steady states on the same carbon source and when the two different carbon sources were compared. However, the gels run from the samples collected within the 1 h transition time after the switch to anaerobiosis increased the number of replica gels analysed and showed the consistency of the quantification. About 50 spots were found to differ in abundance when glucose and xylose samples were compared, and 30 when aerobic and anaerobic samples were compared.

Protein spots showing consistent differences in intensity between different conditions (aerobic or anaerobic glucose or xylose chemostat cultivations) were identified by mass spectrometric peptide mass mapping or by internal peptide sequencing. Some constant spots were also identified. Protein identifications were verified by comparisons with theoretical molecular weights and isoelectric points. We identified 22 proteins that show a clear difference in abundance between glucose and xylose as carbon sources (Table 2 and Figure 2). We also

identified 12 proteins that responded only to the change in aerobicity in the two chemostat cultivations (Table 3 and Figure 3). These proteins are discussed in detail later. We identified 26 proteins that did not respond to any changes under these cultivation conditions (Table 4).

In the analysis it was also noticed that many proteins appeared in the gels as more than one spot with essentially the same molecular weight but with different pI values and abundance, presumably due to post-translational modifications (Gygi *et al*., 2000; see Tables 2, 3 and 4, Figure 1). Proteins for which two or more spots were positively identified by MS analyses include cytoplasmic aldehyde dehydrogenase (Ald6p), enolase 2 (Eno2p), alcohol dehydrogenase 2 (Adh2p) and 3-isopropylmalate dehydrogenase (Leu2p), all detected in three different spots, alcohol dehydrogenase 1 (Adh1p), seen as four spots and, adenosine kinase (Ado1p), heat shock protein Sti1p, translation initiation factor eIF-5A (Hyp2p) and 3-phosphoglycerate kinase (Pgk1p) detected as two separate spots. All these

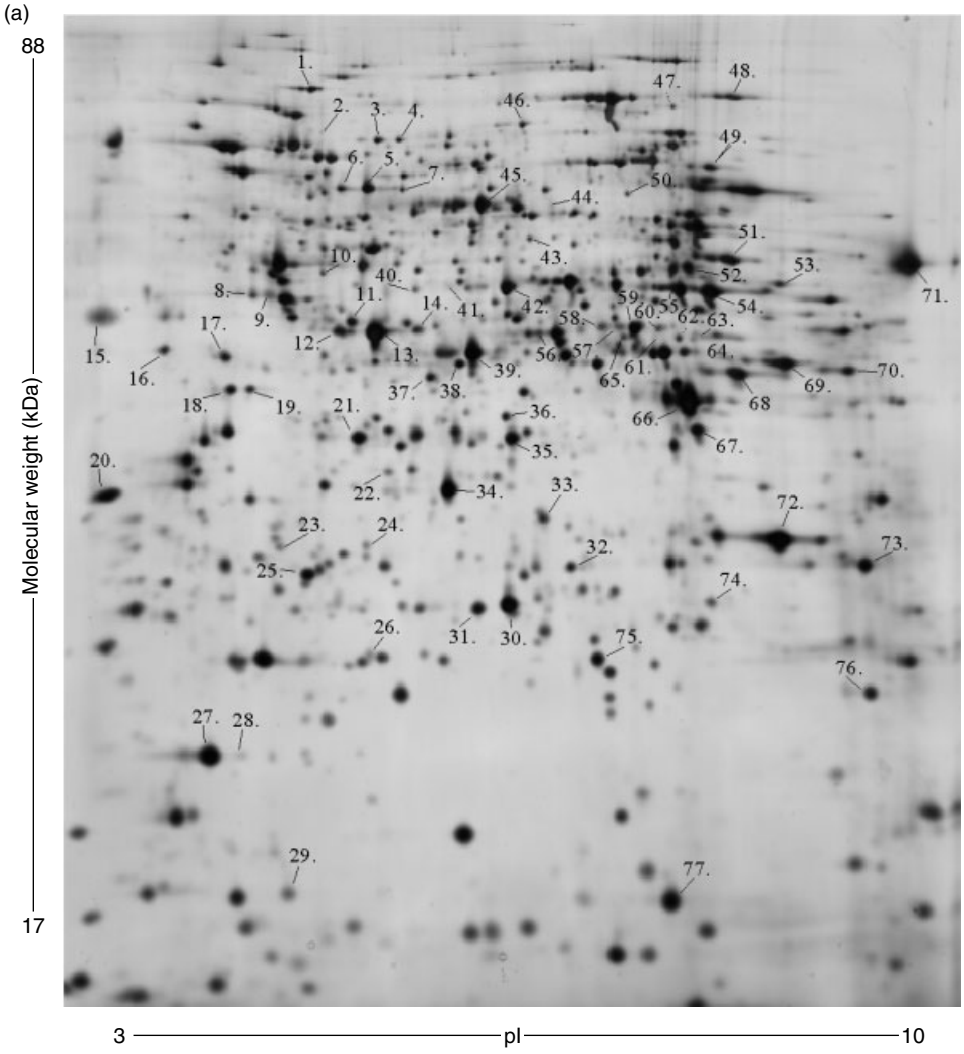

Figure 1. (A) Silver-stained 2D-PAGE pattern of the protein extract from recombinant *S. cerevisiae* grown aerobically on glucose. The horizontal axis is the isoelectric focusing dimension from pH 3 (left) to pH 10 (right). The vertical axis is polyacrylamide gel (12%) dimension from 90 kDa to 15 kDa. (B) The protein spots of Ald6p, Adh2p, Ald4p and Gpp1 from the gels run from the different chemostat conditions (aerobic 10 g/l glucose, aerobic 3 g/l glucose + 27 g/l xylose, anaerobic 10 g/l glucose and anaerobic 3 g/l glucose + 27 g/l xylose). Spot numbers refer to Figure 1A and Table 2

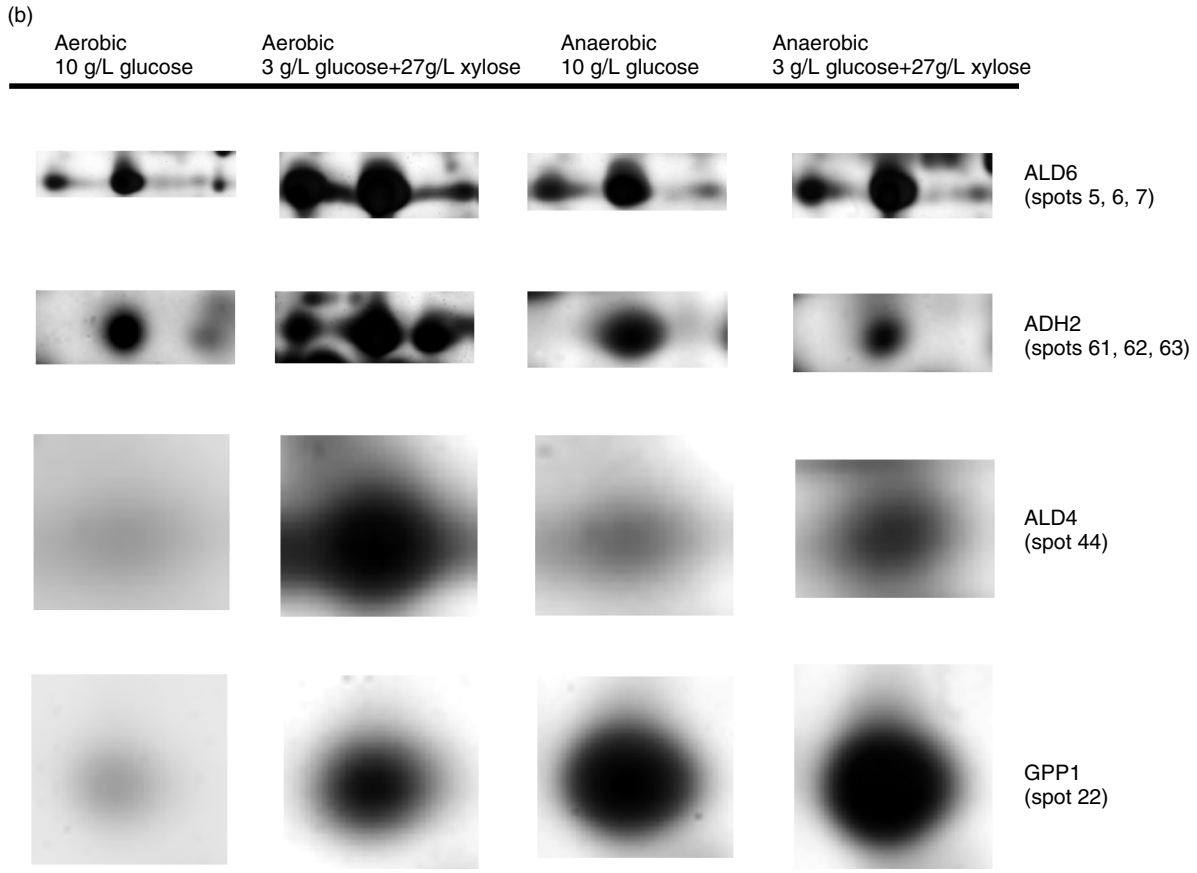

Figure 1. Continued

different pI forms of proteins mentioned here have already been detected in earlier 2-DE gel studies of *S. cerevisiae* (Gygi *et al*., 1999b; Perrot *et al*., 1999). Perhaps surprisingly, for all these proteins the relative amounts of the different pI forms apparently did not change with the culture conditions in our experiments. Thus, even if these modifications have some regulational purposes, they are insensitive to the changes in conditions we have used (glucose/xylose, aerobic/anaerobic).

Spots 29, 10 and 24 corresponded to fragments of Hyp2p, heat shock protein Ssa1p and pyruvate decarboxylase Pdc1p, respectively (see Figure 1, Tables 2 and 4). No major proteolysis was observed in the gels analysed and it is a possibility that these protein fragments occur naturally in yeast cells due to the natural turnover of proteins. Also other studies have reported on occurrence of protein fragments in two-dimensional gels (Perrot *et al*., 1999).

In this study, we have identified five protein spots that are novel identifications in the proteome of *S. cerevisiae*. These proteins are fumarase (Fum1p), a component of the glycine decarboxylase complex Gcv1p, YMR315W, YBL064C and the mitochondrial glycerol-3-phosphate dehydrogenase (Gut2p) (for review, see yeast protein map **http://www.ibgc.u-bordeaux2.fr/YPM/**; also Gygi *et al*., 1999b; Perrot *et al*., 1999). All identifications are shown in Tables 2, 3 and 4 and in Figure 1.

Proteins responding to carbon source

The 22 identified proteins responding to changed carbon source (xylose or glucose) were sorted into six different categories (see Table 2 for identity, Figure 1 for position and Figure 2 for quantity in different samples).

Table 2. Identified proteins responding to change in carbon source. The spot numbers refer to Figure 1 (see also Figure 2 for quantitation). The two right-most columns indicate the mode of response on xylose relative to glucose under aerobic and anaerobic conditions (up, down or same)

				Quantity on xylose relative to quantity on glucose	
Spot number	**Gene[a]**	**Description**	**pI[b]/MW[c]**	**Aerobic**	**Anaerobic**
Proteins of central carbon metabolism					
11	*GPD1*	Glycerol-3-phosphate dehydrogenase	5.27/43.2	Same	Down
5, 6, 7	*ALD6*	Aldehyde dehydrogenase, cytoplasmic ($NADP^+$)	5.38/54.4	Up	Up
22	*GPP1*	DL-glycerol-3-phosphatase	5.43/27.8	Up	Up
44	*ALD4*	Aldehyde dehydrogenase, mitochondrial [$NAD(P)^+$]	5.88/54.1	Up	Same
40, 41, 42	*ENO2*	Enolase 2	5.82/46.8	Up	Up
61, 62, 63	*ADH2*	Alcohol dehydrogenase 2	6.51/36.6	Up	Down
Proteins of TCA cycle and energy generation					
52	*FUM1*	Fumarase	7.00/50.1	Down	Down
50	*CYB2*	L-lactate cytochrome *c* oxidoreductase cytochrome b_2	6.36/56.6	Up	Same
67	*MDH1*	Malate dehydrogenase, mitochondrial	7.00/33.8	Down	Down
68	*IDH2*	Isocitrate dehydrogenase (NAD^+) subunit 2	7.36/37.8	Down	Down
69	*IDH1*	Isocitrate dehydrogenase (NAD^+) subunit 1	8.13/38.0	Down	Down
76	*ATP7*	F-type H+-transporting ATPase d chain	9.08/19.7	Down	Down
Proteins of amino acid metabolism					
47	*LYS4*	Homoaconitate hydratase	7.23/75.1	Up	Up
53	*GCV1*	Component of glycine decarboxylase complex, mitochondrial	9.02/44.3	Down	Down
Proteins related to nucleotide metabolism					
18, 19	*ADO1*	Adenosine kinase	5.05/36.2	Down	Down
31	*ADK1*	Adenylate kinase	5.97/24.1	Down	Down
Heat shock proteins					
2	*SSE1*	Heat shock protein of the HSP70 family	5.02/77.2	Up	Same
25	*HSP26*	Heat shock protein 26	5.44/23.7	Up	Down
46	*HSP78*	Heat shock protein 78 of the ClpB family of ATP-dependent proteases	6.13/85.1	Down	Down
Other proteins					
56	*YHB1*	Flavohaemoglobin	6.04/44.6	Down	Down
65	*YMR315W*	Unknown, putative oxidoreductase	6.40/38.1	Up	Up
74	*YBL064C*	Mitochondrial thiol peroxidase	9.09/29.5	Down	Same

[a] Gene names according to SGD; **http://genome-www4.stanford.edu/cgi-bin/SGD/locus.pl**
[b] Computed in Swiss Prot from the complete sequence; **http://www.expasy.ch/sprot/**
[c] Predicted mature values in kDa according to YPD; **http://www.proteome.com/databases/index.html**

Carbon source-responding proteins related to central carbon metabolism

The most significant changes in protein quantities between glucose- and xylose-grown cells were detected in proteins belonging to this category. The proteins identified were glycerol-3-phosphate dehydrogenase isoenzyme 1 (Gpd1p), DL-glycerol-3-phosphate phosphatase isoenzyme 1 (Gpp1p), enolase 2 (Eno2p), alcohol dehydrogenase 2 (Adh2p), and both mitochondrial and cytoplasmic

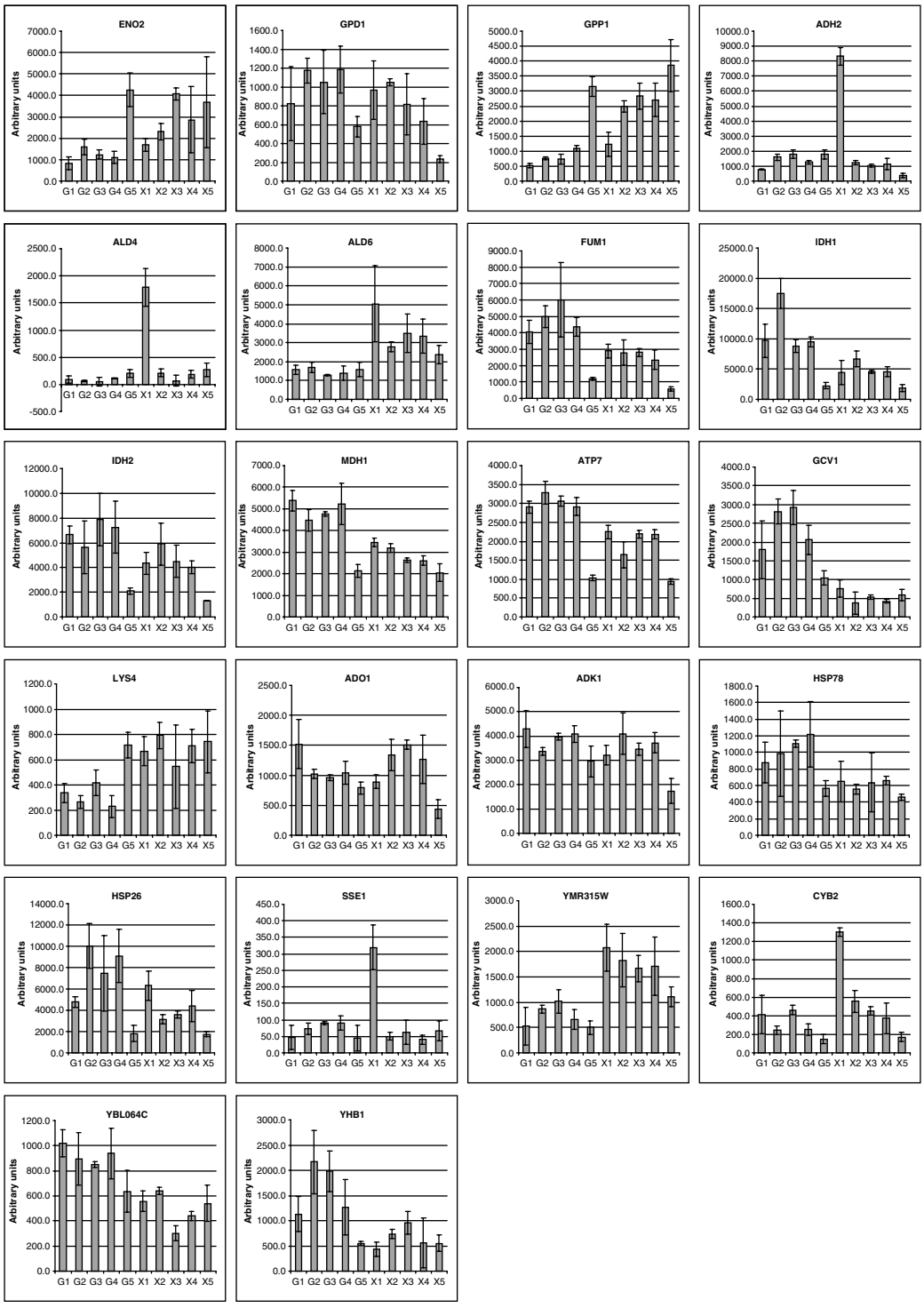

Figure 2. Quantification of protein expression of xylose-responding protein spots from Figure 1 and Table 2. Spots in gel images were quantified as described in Materials and methods. The vertical axis represents arbitrary units of expression. Histograms indicate the mean quantitative values and standard deviations calculated from the replica gels. On the *x* axis samples are in the following order: G1, aerobic glucose chemostat; G2, G3 and G4, 5, 30 and 60 min after the switch-off of oxygen; G5, anaerobic glucose chemostat; X1, aerobic xylose chemostat; X2, X3 and X4, 5, 30 and 60 min after the switch-off of oxygen; and X5, anaerobic xylose culture

Table 3. Identified proteins responding to the level of oxygen. Spot numbers refer to Figure 1 (see Figure 3 for quantitation). The right-most column indicates the mode of response aerobically relative to anaerobic conditions (up, down or same)

Spot number	Gene[a]	Description	pI[b]/MW[c]	Quantity aerobically compared to quantity anaerobically
3, 4	*STI1*	Heat shock protein	5.42/66.3	Up
16	*SGT2*	Unknown, has 32% identity to STI1	4.63/37.1	Up
17	*YIL041W*	Hypothetical ORF	4.71/36.6	Up
26	*PRE3*	20S proteasome subunit	5.73/23.5	Up
27, 28, 29 (frag.)	*HYP2*	Translation initiation factor eIF-5A	4.77/17.0	Up
32	*YMR226C*	Protein with similarity to insect-type short-chain alcohol dehydrogenase	6.59/29.0	Up
33	*GPP2*	DL-glycerol-3-phosphatase	5.97/27.7	Up
36	*YDL124W*	Hypothetical ORF, has similarity to aldo/keto reductases	5.97/35.4	Same/down
43	*FRDS1*	Cytoplasmic soluble fumarate reductase	6.11/50.7	Down
49	*GUT2*	Mitochondrial FAD-dependent glycerol-3-phosphate dehydrogenase	7.14/68.4	Up
57, 58, 59, 60	*ADH1*	Alcohol dehydrogenase 1	6.30/36.7	Down
75	*SOD2*	Manganese superoxide dismutase	6.29/23.1	Up

[a] Gene names according to SGD; **http://genome-www4.stanford.edu/cgi-bin/SGD/locus.pl**
[b] Computed in SwissProt from the complete sequence; **http://www.expasy.ch/sprot/**
[c] Predicted mature values in kDa according to YPD; **http://www.proteome.com/databases/index.html**

acetaldehyde dehydrogenases, Ald4p and Ald6p, respectively. There are clearly three classes of proteins with respect to the pattern of changes observed.

1. *Significantly decreased levels on anaerobic xylose.* The level of Gpd1p remained relatively constant during the glucose chemostat cultivation; however, it had decreased to one half in the anaerobic steady state. In turn, the amount of Gpd1p in the anaerobic xylose culture was only one-third of the amount in the corresponding glucose steady state and also significantly lower compared to the aerobic xylose cultivation.
2. *Increased levels on anaerobic cultivations and overall on xylose.* The amount of Gpp1p was three- to four-fold higher in the anaerobic steady states on both carbon sources in comparison with the corresponding aerobic steady states. Interestingly, the response to oxygen depletion was much faster on xylose. Already within 5 min after the switch-off of oxygen, Gpp1p had reached an about 2.5-fold higher level than that of the aerobic steady state. In addition, Gpp1p level was higher throughout the xylose chemostat cultivation compared to the glucose cultivation, also at the aerobic steady state. In contrast, Gpp2p, the other DL-glycerol-3-phosphatase isoenzyme, responded mainly to oxygen depletion and not significantly to change in the carbon source (see also below; proteins responding to oxygen level). The quantity profiles of Eno2p were very similar to that of Gpp1p; significantly higher levels in anaerobic cultivations, with a quick response to oxygen switch-off on xylose, and overall higher levels on this carbon source.
3. *Increased levels on aerobic xylose and in addition, one member of this class shows overall increase on xylose.* The abundance of three proteins involved in ethanol utilization, Adh2p, Ald4p and Ald6p, was strongly increased in the aerobic steady state on xylose compared to glucose. While the levels of Adh2p and Ald4p remained low on glucose and were strongly decreased on xylose as soon as oxygen was depleted, the level of Ald6p was about three times higher in all anaerobic xylose samples compared to the corresponding samples collected from the glucose culture.

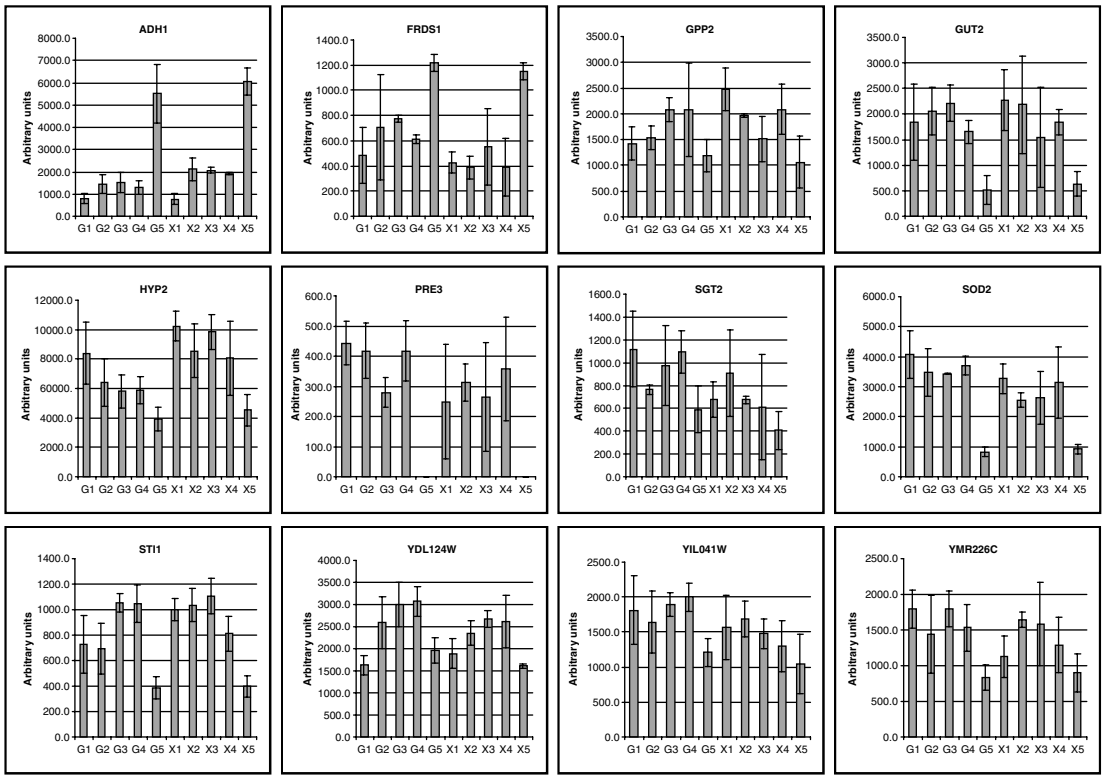

Figure 3. Quantification of protein expression of protein spots responding to the change in aerobicity from Figure 1 and Table 3. Spots in gel images were quantified as described in Materials and methods. The vertical axis represents arbitrary units of expression. Histograms indicate the mean quantitative values and standard deviations calculated from the replica gels. On the *x* axis samples are in the following order: G1 aerobic glucose chemostat; G2, G3 and G4, 5, 30 and 60 min after the switch-off of oxygen; G5, anaerobic glucose chemostat; X1, aerobic xylose chemostat; X2, X3 and X4, 5, 30 and 60 min after the switch-off of oxygen; and X5, anaerobic xylose culture

Carbon source-responding proteins of tricarboxylic acid cycle and energy generation

Six protein spots were identified as two subunits of mitochondrial NAD^+-dependent isocitrate dehydrogenase (Idh1p and Idh2p), mitochondrial malate dehydrogenase (Mdh1p), fumarase (Fum1p), L-lactate cytochrome *c* oxidoreductase cytochrome b_2 (Cyb2p), and subunit 7 of F0-ATP synthase (Atp7p). These protein spots, except Cyb2p, behaved quantitatively in a similar fashion. Anaerobic steady-state levels on both carbon sources were roughly equal but clearly lower than the corresponding steady-state aerobic levels. More interestingly in respect to the two carbon sources, they all had an overall lower level in xylose samples, in particular Fum1p and Idh1p. In turn, the amount of Cyb2p was shifted up on the aerobic xylose cultivation more than two-fold, whereas its level was otherwise relatively low and constant, independent of the carbon source.

Carbon source-responding proteins of amino acid metabolism

Two proteins of this category responded to the two different carbon sources studied. The quantity of homoaconitase hydratase (Lys4p) was elevated in anaerobic glucose cultivation and was at this high level also from the beginning to the end of the xylose cultivation. The other protein, (Gcv1p) is a component of the glycine decarboxylase complex. The level of this protein was reduced during anaerobic cultivation on glucose compared to aerobic conditions. On xylose, the amount was low throughout the xylose cultivation.

Table 4. Identified proteins found at constant abundance in this study. Protein spots numbered accordingly in Figure 1

Spot number	Gene[a]	Description	pI[b]/MW[c]
1	*HIS4*	Histidinol dehydrogenase	5.13/87.6
8	*TIF2*	Translation initiation factor 4A	4.99/44.6
9	*SAM2*	S-adenosylmethionine synthetase 2	5.21/42.1
10 (fragment)	*SSA1*	70 kDa heat shock protein	4.96/69.6
12, 13, 14	*LEU2*	3-Isopropylmalate dehydrogenase	5.61/38.8
15	*PEP4*	Vacuolar proteinase A	4.41/35.7
20	*EFB1*	Translation elongation factor EF-1β	4.30/22.6
21	*IPP1*	Inorganic pyrophosphatase	5.46/32.2
23	*YLR301W*	Protein of unknown function	5.04/27.4
30	*TPI1*	Triosephosphate isomerase	5.84/26.7
34	*ASC1*	Ribosomal protein of the 40S ribosomal subunit that influences translational efficiency and cell size	5.87/34.7
35	*XYL1*	D-Xylose reductase of *Pichia stipitis*	5.76/35.9
37	*ARA1*	Subunit of $NADP^+$-dependent D-arabinose dehydrogenase	5.76/38.3
38	*XYL2*	Xylitol dehydrogenase of *Pichia stipitis*	5.76/38.5
39	*FBA1*	Fructose-bisphosphate aldolase II	5.58/39.6
48	*ACO1*	Aconitate hydratase	7.07/82.8
45, 24 (fragment)	*PDC1*	Pyruvate decarboxylase isozyme 1	5.97/61.5
51	*SHM2*	Serine hydroxymethyltransferase	7.25/52.1
54, 55	*PGK1*	3-phosphoglycerate kinase	7.11/44.6
64	*LYS12*	Homo-isocitrate dehydrogenase	8.24/40.1
66	*TDH2/TDH3*	Glyceraldehyde 3-phosphate dehydrogenase 2/3	6.72/35.7
72	*POR1*	Outer mitochondrial membrane porin	7.94/30.4
73	*GPM1*	Phosphoglycerate mutase	8.95/27.5
71	*TEF1/TEF2*	Translational elongation factor EF-1α	9.27/50.0
70	*BAT1*	Mitochondrial branched-chain amino acid transaminase	7.83/38.7
77	*CPH1*	Cyclophilin (peptidylprolyl *cis–trans* isomerase or PPIase)	6.75/17.3

[a] Gene names according to SGD; **http://genome-www4.stanford.edu/cgi-bin/SGD/locus.pl.**
[b] Computed in Swiss Prot from the complete sequence; **http://www.expasy.ch/sprot/**
[c] Predicted mature values in kDa according to YPD; **http://www.proteome.com/databases/index.html**

Carbon source-responding proteins related to nucleotide metabolism

The two proteins belonging to this category were adenosine kinase (Ado1p) and adenylate kinase (Adk1p). They were both relatively abundant protein spots and steadily expressed throughout the cultivations but nevertheless had lower abundance anaerobically in the xylose cultivation.

Carbon source-responding heat shock proteins

Hsp78p and Hsp26p were present at lower levels in the anaerobic glucose cultivation, and were present at that or at somewhat higher level during the entire xylose cultivation. In turn Sse1p, a heat shock protein belonging to the Hsp70 family, was strongly induced on the aerobic xylose cultivation, but it remained at very low level at the other cultivation steps.

Other carbon source- responding proteins

Mitochondrial thiol peroxidase YBL064C and yeast flavohaemoglobin (Yhb1p) showed decreased levels in the anaerobic steady state on glucose, and they both were at similar low quantities in the entire xylose cultivation, in particular Yhb1p. In contrast, YMR315W was constantly at a higher level in the xylose cultivation compared to the glucose cultivation. However, in the anaerobic xylose cultivation the amount of YMR315W was only about half of that of the aerobic level.

Proteins responding to oxygen level

Mitochondrial glycerol-3-phosphate dehydrogenase (Gut2p) and mitochondrial manganese superoxide dismutase (Sod2p) had approximately four times lower abundance in the anaerobic cultivations, and the 20S proteasome subunit (Pre3p) could not be detected in anaerobic samples. Furthermore, the heat shock protein Sti1p, and Sgt2p (which has 32% identity to Sti1p but is without any specified function) had a two-fold lower abundance anaerobically compared to aerobic cultures. In addition, Gpp2p, one of the isoforms of DL-glycerol-3-phosphatase, and the translation initiation factor Hyp2p also had about two-fold lower protein amounts anaerobically compared to the aerobic cultivations. Some of these proteins also appeared to have slightly different abundances on the two carbon sources studied. Sgt2p had somewhat reduced levels in xylose samples, whereas Gpp2p showed a slightly higher level aerobically on xylose in comparison with glucose. In addition, the response to oxygen depletion seems slightly faster on xylose than on glucose with Gut2 and Gpp2 proteins.

The quantity of YDL124W, a hypothetical ORF with significant homology to the gene encoding a glycerol dehydrogenase of *Aspergillus niger*, did not differ between the aerobic and anaerobic cultivations, but instead seemed to respond to depletion of oxygen by a transient increase in the protein level right after the switch from aerobic to anaerobic conditions. YMR226C, a protein with similarity to short-chain dehydrogenases or reductases, had about two-fold lower abundance anaerobically in the glucose cultivation. However, in the aerobic xylose cultivation its abundance was only slightly higher compared to the anaerobic glucose cultivation, and on xylose it showed a transient increase in abundance in response to oxygen depletion, in a similar fashion to YDL124W. Furthermore, YIL041W had about one-third lower abundance anaerobically on both carbon sources.

In addition, cytoplasmic fumarate reductase (Frds1p) and alcohol dehydrogenase 1 (Adh1p) had about two- and three-fold increase in abundance, respectively, during anaerobic growth compared with aerobic conditions on both carbon sources. The changes detected between aerobic and anaerobic conditions at the protein level of Adh1p, Frds1p, Gpp2p, Gut2p, Hyp2p, Sod2p, and Sti1p are in accordance with the results of a transcriptional analysis of aerobic and anaerobic chemostat cultures of *S. cerevisiae* (ter Linde, *et al*., 1999; see also **http://www.imp.leidenuniv.nl/ yeast/search.htm**).

Discussion

Efficient utilization of the xylose component of carbohydrate feedstocks in addition to hexoses would make it possible to reduce the cost of bioethanol production. Thus, the xylose metabolic pathway has been studied intensively over the years in various naturally xylose-utilizing yeasts, as well as in recombinant *S. cerevisiae* strains that have been constructed in order to obtain strains that are suitable for industrial processes. In *S. cerevisiae*, despite the recombinant xylose pathway, the rate of xylose utilization and the yield of ethanol are still low and further strain development is needed.

We report here the first proteome-wide study of xylose-fermenting recombinant *S. cerevisiae*, aiming at a broad insight to the effects of xylose on cellular metabolism. The strain H2490 was cultivated in chemostats on xylose as the main carbon source, and for comparison on glucose under both aerobic and anaerobic conditions for seven and six residence times, respectively. Clear changes in the quantities of 22 identified proteins were seen between xylose and glucose samples harvested from these chemostat cultivations. The cellular functions that were most affected are related to glycerol metabolism, ethanol consumption and mitochondrial metabolism.

Proteins of glycerol metabolism

As expected, changes between xylose and glucose were seen in proteins related to glycerol metabolism, since NADH-consuming production of glycerol has an important role in balancing the intracellular redox potential. Glycerol metabolism in *S. cerevisiae* has been extensively studied and reviewed, e.g. by Bakker *et al*. (2001). Glycerol-3-phosphate dehydrogenase (Gpd) and DL-glycerol-3-phosphate phosphatase (Gpp), which catalyse glycerol synthesis from dihydroxyacetone phosphate, are both encoded by two isogenes. These isoforms have different roles under osmotic and anaerobic stress conditions. The isoforms encoded by *GPD1*

and *GPP2* are osmotically induced, while *GPD2* and *GPP1* are induced under anaerobic conditions (Albertyn *et al*., 1994; Ansell *et al*., 1997; Costenoble *et al*., 2000; Påhlman *et al*., 2001; ter Linde *et al*., 1999). In our proteome study, Gpd1p had reduced levels under anaerobicity, in particular on xylose, and the amounts of Gpp2p were also lower under oxygen depletion. Further, Gpp1p had strongly elevated levels in anaerobic steady states, well in accordance with previous studies. Interestingly, in the xylose culture, Gpp1p responded more quickly to the switch-off of oxygen than it did in the glucose culture. This may be due to an increased demand for NADH oxidation, even aerobically, because of the NAD^+-consuming XDH reaction in the xylose pathway. This possible co-factor demand was not, however, seen as an increased level of the reducing enzyme Gpd1p, and Gpd2p, the isoenzyme that is more probably responding in concert with Gpp1p, was not identified amongst the proteins responding differently to either the carbon source or oxygen level. Additionally, in the anaerobic xylose culture, where the level of Gpp1p was highest, the amount of Gpd1p was lowest, giving support to the idea that Gpd1p indeed does not play a significant role in anaerobic redox control. This seems to be true also with Gpp2p, as its level in anaerobic steady states was the lowest in comparison with the other samples. In summary, even though seen only for the DL-glycerol-3-phosphatases, xylose seems to activate the cellular pathway where oxidation of NADH is carried out, as a response for the elevated NADH generation during xylose metabolism in comparison with glucose metabolism.

In addition to glycerol synthesis, cells have aerobically the option to maintain their cytoplasmic NAD/NADH balance by transfer of reducing equivalents into the mitochondrial electron transport chain (de Vries and Marres, 1987). This can be achieved either via the external NADH dehydrogenases facing the outer side of the inner mitochondrial membrane, or by shuttle systems such as the glycerol-3-phosphate (G3P) shuttle. In the G3P shuttle, G3P, formed by reduction of dihydroxyacetone phosphate and concomitant oxidation of NADH, passes through the outer mitochondrial membrane. G3P is then re-oxidized to dihydroxyacetone phosphate by the FAD-dependent glycerol-3-phosphate dehydrogenase (Gut2p) located on the outer side of the inner membrane of mitochondria (Bakker *et al*., 2001; Larsson *et al*., 1998). *GUT2* is aerobically induced according to the transcriptional profiling data from aerobic and anaerobic glucose-limited chemostat cultures of yeast (ter Linde *et al*., 1999). In addition, it has been reported that the dehydrogenase catalysing the cytosolic reaction of the G3P shuttle is encoded by the *GPD1* gene (Larsson *et al*., 1998). These data are in agreement with the proteome profiles of Gut2p and Gpd1p in our study, as we detected a two- and four-fold reduction in the abundance of Gpd1p and Gut2p, respectively, in the fully anaerobic cultures on both carbon sources (Figures 2 and 3). On xylose, shuttles like the G3P shuttle could alleviate the NAD^+ shortage and also explain the almost equal specific glycerol production rates on xylose and glucose (see Table 1); Pitkänen *et al*., in press). However, according to our data, the Gut2p involved in the G3P shuttle has similar abundance on both xylose and glucose, which does not support the suggestion that the shuttle would be more active on xylose.

In *S. cerevisiae* the NAD/NADH and NADP/NADPH pools constitute distinct redox couples, due to the absence of a transhydrogenase activity in yeast that would be able to convert NADH to NADPH. The existence of systems serving as transhydrogenase-like activities has, however, been postulated. A study of the proteome in 1.4 M NaCl (Norbeck and Blomberg, 1997) suggested that coupling of glycerol formation and degradation could provide the cell with an enzymatic cycle functioning as a transhydrogenase. Actually, it was proposed that the hypothetical protein encoded by ORF *YDL124W*, with significant homology to a glycerol dehydrogenase of *Aspergillus niger*, is one of the candidates for a yeast glycerol dehydrogenase taking part in this kind of a cycle (Norbeck and Blomberg, 1997). However, these authors found no transcripts for *YDL124W* under any of the growth conditions studied. We were able to identify the Ydl124w protein in our proteome, and in our study it is classified to the group of oxygen-responding proteins moderately upregulated immediately after the switch-off of oxygen on both carbon sources (see Figure 3). However, the level of Ydl124w protein returned to the aerobic level within the five residence times needed to achieve the anaerobic metabolic steady state. Thus, although Ydl124w protein clearly responds to oxygen depletion and does so very rapidly (within

5 min; Figure 3), and is therefore likely to participate in the adaptation to anaerobicity, our study does not support that it would be needed for a long-term redox balancing under anaerobic conditions. Further, there is no difference in the protein amount or response between the two carbon sources studied.

Aerobic increase of Adh2p, Ald4p, Ald6p and Cyb2p levels on xylose

The higher abundance of alcohol dehydrogenase isoenzyme Adh2p and the acetaldehyde dehydrogenases Ald6p and Ald4p during aerobic growth on xylose-containing media is, according to our hypothesis, related to the increased NADPH co-factor demand due to XR reaction in the xylose pathway. The increased levels of Adh2p and acetaldehyde dehydrogenases in the aerobic xylose cultures also render support to the fact that, under aerobic conditions on xylose, acetate and ethanol are used as co-substrates for growth, along with xylose (Meinander and Hahn-Hägerdal, 1997).

While Adh1p reduces acetaldehyde to ethanol and is responsible for ethanol production, which under anaerobic conditions is used for NAD^+ regeneration, Adh2p oxidizes ethanol to acetaldehyde. NADPH or NADH is regenerated when acetaldehyde is further oxidized to acetate by acetaldehyde dehydrogenases. Acetaldehyde thus produced is further metabolized by more than one optional pathway, either in the cytosol or in the mitochondria, all serving either in balancing the redox pools or producing reducing equivalents for the production of ATP.

1. Acetaldehyde can freely enter the mitochondria and serve as a substrate for the mitochondrial alcohol dehydrogenase isozyme Adh3p, to form an ethanol–acetaldehyde shuttle that is used to export redox equivalents from the mitochondrial matrix to the cytosol. It is suggested that, in anaerobic cultures, this shuttle may play a key role in reoxidation of mitochondrial NADH formed by assimilatory reactions that take place in mitochondria also under anaerobic conditions (Bakker *et al*., 2000, 2001). On xylose this kind of shuttle may play a role in balancing the NAD^+/NADH levels of the cell. The shuttle is in principle reversible, thus ethanol produced in the cytosol could alternatively enter the mitochondria, and Adh3p will oxidize ethanol to acetaldehyde, with concomitant reduction of NAD^+. However, as there is no phenotype aerobically for the *ADH3* deletion mutant, no evidence of a role for the ethanol–acetaldehyde cycle under aerobic growth exists (Bakker *et al*., 2000). Adh3p was not identified in our study amongst the proteins responding differently to the carbon source or oxygen level.
2. Based on our proteomics results on xylose, however, a more likely fate of acetaldehyde produced by the action of Adh2p (or by Pdc1p) is to serve as a substrate for acetaldehyde dehydrogenases. NADPH or NADH is regenerated when acetaldehyde is oxidized to acetate by acetaldehyde dehydrogenases. The existence of at least five acetaldehyde dehydrogenase isoforms with different co-factor specificities, known to be able to complement each other, supports the idea of a role for these isoenzymes in maintaining the cytosolic and mitochondrial redox co-factor pools. Cytosolic Ald6p, the level of which is clearly elevated in the xylose chemostat of our study (Figures 1b, 2), is the major isoform of acetaldehyde dehydrogenases and it almost exclusively uses $NADP^+$ (Dickinson, 1996; Remize *et al*., 2000; Wang *et al*., 1998). Ald6p has been shown to be functional in both glucose- and ethanol-grown yeast cells (Remize *et al*., 2000). Ald6p is responsible for the cytosolic conversion of acetaldehyde to acetate, the latter acting as substrate for acetyl-CoA synthase, producing the precursor acetyl-CoA, needed for glyoxylate cycle and lipid biosynthesis in the cytosol. Ald6p is thus a member of the so-called cytosolic pyruvate dehydrogenase bypass, providing the cytosolic compartment with acetyl-CoA. In addition, the physiological role of the Ald reaction is very likely the regeneration of reducing equivalents, the demand for which is increased during xylose metabolism via the XR reaction.

In contrast, mitochondrial Ald4p that is able use both NAD^+ and $NADP^+$ does not seem to have a role in acetate production in fermentative metabolism (Remize *et al*., 2000). The elevated levels of this isoenzyme in aerobic xylose culture of our study (Figures 1b, 2) gives support to our hypothesis that xylose is not readily regarded as a fermentable carbon source in the yeast cell. Recently, an interesting physiological

role for Ald4p was proposed as the key player in the so-called mitochondrial pyruvate dehydrogenase bypass (Boubekeur *et al*., 1999, 2001). Acetaldehyde produced in the cytosol enters the mitochondria, where it is oxidized to acetate with concomitant formation of NADH, which in turn serves to produce ATP. Further, Ald4p increases the overall production of NADH in the cell, as it acts as an acetaldehyde pump, and this NAD^+-reducing flux increases both ATP production and biosynthetic pathways. Alternatively, one can envision a role for Ald4p in ethanol consumption in the mitochondria. Ethanol produced in the cytosol could enter the mitochondria and be oxidized to acetaldehyde, and further to acetate, by mitochondrial Adh and Ald isozymes to produce NADH for energy metabolism (Bakker *et al*., 2001).

As increased acetate levels on xylose compared to glucose were not detected in the growth medium (see Table 1), the acetate possibly produced must have been converted by acetyl-CoA synthetase to acetyl-CoA to serve as a precursor, e.g. in the TCA cycle and lipid metabolism and glyoxylate cycle. In summary, increased levels of Adh2p, and the two Ald isoenzymes are indicative of increased demand for redox balancing and energy metabolism during xylose consumption by the cells. As shown by metabolic flux analysis of xylose metabolism (e.g. Pitkänen *et al*., submitted), a cycle of carbon back to PPP at the level of glucose-6-P to produce NADPH for the XR reaction results in reduced flux to pyruvate, and thus in a reduced formation of NADH for the energy metabolism in aerobic chemostat cultures.

In yeast, the utilization of L (+)-lactate requires mitochondrial Cyb2p, which oxidizes L(+)-lactate to pyruvate by coupling L-lactate dehydrogenation to cytochrome *c* reduction. Besides repression in anaerobiosis on non-repressing carbon sources such as galactose and raffinose, the *CYB2* gene is reported to be highly induced by non-fermentable carbon sources such as ethanol, glycerol and, particularly, by lactate (Guiard, 1985; Lodi and Guiard, 1991; Ramil *et al*., 2000). It is also fully repressed by glucose and inhibited by the absence of heme biosynthesis (Lodi and Guiard, 1991). Here we show higher levels of Cyb2p also in aerobic xylose cultures. This strengthens our hypothesis that the utilization of xylose in aerobic conditions triggers responses in the cell that are similar to those found on non-fermentable carbon sources. As ethanol is likely to be utilized (and also glycerol and acetate) as a co-substrate along with xylose, the co-metabolism of these non-fermentable end products may further increase the signal for *CYB2* expression. Increased levels of Adh2p, Ald4p and Cyb2p on aerobic xylose culture in our study are in accordance with results obtained from DNA microarray analysis of transcription of *S. cerevisiae* in aerobic and anaerobic glucose-limited chemostat cultures (ter Linde *et al*., 1999). The levels of most of the proteins identified in our proteome study did not change significantly after switch-off of oxygen within the 1 h time range; however, Adh2p, Ald4p and (to a lesser extent) Cyb2p made an exception by almost disappearing within 5 min after the switch (Figure 2). Our results also suggest that downregulation of these genes at the transcriptional level probably takes place very rapidly and that it must be combined to surprisingly fast proteolytic degradation. For example, the well-studied glucose-induced degradation of fructose-1,6-bisphosphatase in yeast results in substantially decreased protein amounts only after a 30 min time period (Horak *et al*., 2002).

Mitochondrial proteins

Under anaerobic conditions, oxidation of intramitochondrial NADH by the respiratory chain is abolished and, as a result, the function of the TCA cycle is diminished as well. In our study we see decreased levels of mitochondrial proteins in anaerobic cultivations on both carbon sources (Figure 2). This is not surprising as, under anaerobic conditions, cells switch to completely fermentative energy metabolism, and the role of mitochondrial functions reduces to assimilatory metabolism. More surprising, however, is the observation that all seven of the identified mitochondrial proteins also show decreased levels on xylose in aerobic cultures. We would anticipate them to be at roughly the same level as in glucose-grown but derepressed cells (for the reasoning of the derepression state in our glucose-limited chemostat cultures, see section on Chemostat cultivations and experimental design, end of first paragraph). This is against our hypothesis of xylose being a non-fermentable carbon source, as growth on xylose should in contrast then result in elevated mitochondrial functions. Interestingly, the metabolic flux analysis of

metabolism during growth on xylose gave consistent results, showing substantially decreased mitochondrial fluxes (Pitkänen *et al*., in press).

The reactions from glucose 6-phosphate to ribulose 5-phosphate in the oxidative pentose phosphate pathway are important for regeneration of the cytosolic NADPH. The increased need for NADPH on xylose due to the XR reaction requires conversion of fructose 6-phosphate to glucose 6-phosphate and may create a cycle around the glycolysis and pentose phosphate pathway, as first suggested by Bruinenberg *et al*. (1983). As mentioned previously, such a cycle during xylose metabolism is suggested by metabolic flux analysis (Pitkänen *et al*., in press; Wahlbom *et al*., 2001). The cycling in the upper part of glycolysis may explain the increased enolase (Eno2p) levels that we see on aerobic and anaerobic xylose cultures, as high levels of glucose 6-phosphate induce Eno2p activity (Müller *et al*., 1995).

Increase of YMR315W abundance on xylose

Among proteins identified, the abundance of YMR315W is most markedly increased in xylose-containing medium in all five samples taken from the different time points of the culture (Figure 2). YMR315W is a protein of unknown function, but it has a weak similarity to glucose-fructose oxidoreductase of *Zymomonas mobilis*. It has also 31% identity to two protein sequences of *Schizosaccharomyces pombe*, coding for putative oxidoreductases SPAC26145.09c and SPBC115.03, and 26% identity to a dihydrodiol dehydrogenase of *Sz. pombe.* Glucose-fructose oxidoreductase from Z. *mobilis* converts glucose and fructose to gluconolactone and sorbitol. The enzyme contains a non-dissociable $NADP^+$, which transfers reducing equivalents between glucose and fructose (Kanagasundaram and Scopes, 1992).

A further indication for a role of YMR315W in xylose utilization is that a homologue of YMR315W from the xylose-utilizing fungus *Trichoderma reesei* (*Hypocrea jecorina*) was found in our laboratory in a random cDNA bank screen for clones enhancing growth on xylose of the recombinant xylose-metabolizing *S. cerevisiae* (unpublished results). The function of this putative oxidoreductase in yeast is still unknown, but it clearly seems to be related to xylose consumption. Interestingly, D-xylose is a substrate of the glucose-fructose oxidoreductase of *Z. mobilis* (Zachariou and Scopes, 1986).

The significant advantage of the 2-DE gel proteomic technique is that it can reveal changes in protein abundances not predicted by some *a priori* hypotheses. Our studies revealed several expected, but also interesting unexpected, responses to xylose as the carbon source and to aerobic vs. anaerobic conditions. Many of our findings are related to the redox balance and/or energy metabolism of the cell, and especially the reactions around ethanol and acetaldehyde are highly interesting, as shown by the increased amount of Adh2p, Ald4p and Ald6p in the xylose culture. Another particularly interesting observation was the decreased amounts of proteins of the TCA cycle in xylose-grown cells. Presumably, redox balancing during xylose metabolism causes loss of carbon in the futile cycling in the pentose phosphate pathway, resulting in lower flux to pyruvate and hence to the TCA cycle. Thus, alternative ways for co-factor regeneration are of high importance to increase ethanol yields from this pentose sugar. It is evident that xylose, as a non-natural energy and carbon source of *S. cerevisiae*, causes complex metabolic responses in the cell. The changes are not explained solely by glucose derepression taking place in the cells in the absence of glucose, particularly since our glucose reference cultures were in a derepressed state. Further, many of the responses are related to changes caused by typical non-fermentable carbon sources, strengthening our belief that xylose is not readily recognized as a fermentable carbon source by *S. cerevisiae*.

Acknowledgements

Tiina Pakula is acknowledged for collaboration and many fruitful methodological and experimental discussions in the field of proteomics. John Londesborough is warmly thanked for comments on the manuscript. This study was financially supported by the Academy of Finland and the Technology Agency of Finland (Tekes).

References

Albertyn J, Hohmann S, Thevelein JM, Prior BA. 1994. *GPD1*, which encodes glycerol-3-phosphate dehydrogenase, is essential for growth under osmotic stress in *Saccharomyces cerevisiae*,

and its expression is regulated by the high-osmolarity glycerol response pathway. *Mol Cell Biol* **14**: 4135–4144.

Ansell R, Granath K, Hohmann S, Thevelein JM, Adler L. 1997. The two isoenzymes for yeast NAD^+-dependent glycerol 3-phosphate dehydrogenase encoded by *GPD1* and *GPD2* have distinct roles in osmoadaptation and redox regulation. *EMBO J* **16**: 2179–2187.

Bakker BM, Bro C, Kötter P, *et al*. 2000. The mitochondrial alcohol dehydrogenase Adh3p is involved in a redox shuttle in *Saccharomyces cerevisiae*. *J Bacteriol* **182**: 4730–4737.

Bakker BM, Overkamp KM, van Maris AJ, *et al*. 2001. Stoichiometry and compartmentation of NADH metabolism in *Saccharomyces cerevisiae*. *FEMS Microbiol Rev* **25**: 15–37.

Batt CA, Carvallo S, Easson DD, Akedo JM, Sinskey AJ. 1986. Direct evidence for a xylose metabolic pathway in *Saccharomyces cerevisiae*. *Biotechnol Bioeng* **28**: 549–553.

Blackstock WP. 1999. Proteomics: quantitative and physical mapping of cellular proteins. *TIBTECH* **17**: 121.

Boles E, Gohlmann HW, Zimmermann FK. 1996. Cloning of a second gene encoding 5-phosphofructo-2-kinase in yeast, and characterization of mutant strains without fructose-2,6-bisphosphate. *Mol Microbiol* **20**: 65–76.

Boubekeur S, Bunoust O, Camougrand N, Castroviejo M, Rigoulet M, Guerin B. 1999. A mitochondrial pyruvate dehydrogenase bypass in the yeast *Saccharomyces cerevisiae*. *J Biol Chem* **274**: 21 044–21 048.

Boubekeur S, Camougrand N, Bunoust O, Rigoulet M, Guerin B. 2001. Participation of acetaldehyde dehydrogenases in ethanol and pyruvate metabolism in the yeast *Saccharomyces cerevisiae*. *Eur J Biochem* **268**: 5057–5065.

Brejning J, Jespersen L. 2002. Protein expression during lag phase and growth initiation in *Saccharomyces cerevisiae*. *Int J Food Microbiol* **75**: 27–38.

Bruinenberg PM, van Dijken JP, Scheffers WA. 1983. A theoretical analysis of NADPH production and consumption in yeasts. *J Gen Microbiol* **129**: 953–964.

Christianson TW, Sikorski RS, Dante M, Shero JH, Hieter P. 1992. Multifunctional yeast high-copy-number shuttle vectors. *Gene* **110**: 119–122.

Costenoble R, Valadi H, Gustafsson L, Niklasson C, Frazen CJ. 2000. Microaerobic glycerol formation in *Saccharomyces cerevisiae*. *Yeast* **16**: 1483–1495.

de Vries S, Marres CA. 1987. The mitochondrial respiratory chain of yeast. Structure and biosynthesis and the role in cellular metabolism. *Biochim Biophys Acta* **895**: 205–239.

Dickinson FM. 1996. The purification and some properties of the $Mg2^+$-activated cytosolic aldehyde dehydrogenase of *Saccharomyces cerevisiae*. *Biochem J* **315**: 393–399.

Eliasson A, Christensson C, Wahlbom CF, Hahn-Hägerdal B. 2000. Anaerobic xylose fermentation by recombinant *Saccharomyces cerevisiae* carrying XYL1, XYL2, and XKS1 in mineral medium chemostat cultures. *Appl Environm Microbiol* **66**: 3381–3386.

Gavin AC, Bosche M, Krause R, *et al*. 2002. Functional organization of the yeast proteome by systematic analysis of protein complexes. *Nature* **415**: 141–147.

Gietz RD, Sugino A. 1988. New yeast–*Escherichia coli* shuttle vectors constructed with *in vitro* mutagenized yeast genes lacking six-base pair restriction sites. *Gene* **74**: 527–534.

Godon C, Lagniel G, Lee J, *et al*. 1998. The H_2O_2 stimulon in *Saccharomyces cerevisiae*. *J Biol Chem* **273**: 22 480–22 489.

Gottschalk A, Neubauer G, Banroques J, Mann M, Luhrmann R, Fabrizio P. 1999. Identification by mass spectrometry and functional analysis of novel proteins of the yeast [U4/U6.U5] tri-snRNP. *EMBO J* **18**: 4535–4548.

Guiard B. 1985. Structure, expression and regulation of a nuclear gene encoding a mitochondrial protein: the yeast L($^+$)-lactate cytochrome *c* oxidoreductase (cytochrome b_2). *EMBO J* **4**: 3265–3272.

Gygi SP, Corthals GL, Zhang Y, Rochon Y, Aebersold R. 2000. Evaluation of two-dimensional gel electrophoresis-based proteome analysis technology. *Proc Natl Acad Sci USA* **97**: 9390–9395.

Gygi SP, Rist B, Gerber SA, Turecek F, Gelb MH, Aebersold R. 1999a. Quantitative analysis of complex protein mixtures using isotope-coded affinity tags. *Nature Biotechnol* **17**: 994–999.

Gygi SP, Rochon Y, Franza BR, Aebersold R. 1999b. Correlation between protein and mRNA abundance in yeast. *Mol Cell Biol* **19**: 1720–1730.

Haurie V, Perrot M, Mini T, Jeno P, Sagliocco F, Boucherie H. 2001. The transcriptional activator Cat8p provides a major contribution to the reprogramming of carbon metabolism during the diauxic shift in *Saccharomyces cerevisiae*. *J Biol Chem* **276**: 76–85.

Hayes A, Zhang N, Wu J, *et al*. 2002. Hybridization array technology coupled with chemostat culture: tools to interrogate gene expression in *Saccharomyces cerevisiae*. *Methods San Diego CA* **26**: 281–290.

Ho NW, Chen Z, Brainard AP. 1998. Genetically engineered *Saccharomyces* yeast capable of effective co-fermentation of glucose and xylose. *Appl Environm Microbiol* **64**: 1852–1859.

Ho NWY, Chang S-F. 1989. Cloning of yeast xylulokinase gene by complementation in *Escherichia coli* and yeast mutations. *Enzyme Microb Technol* **11**: 417–421.

Ho Y, Gruhler A, Heilbut A, *et al*. 2002. Systematic identification of protein complexes in *Saccharomyces cerevisiae* by mass spectrometry. *Nature* **415**: 180–183.

Horak J, Regelmann J, Wolf DH. 2002. Two distinct proteolytic systems responsible for glucose-induced degradation of fructose-1,6-bisphosphatase and the Gal2p transporter in the yeast *Saccharomyces cerevisiae* share the same protein components of the glucose signaling pathway. *J Biol Chem* **277**: 8248–8254.

Johansson B, Hahn-Hägerdal B. 2002. The non-oxidative pentose phosphate pathway controls the fermentation rate of xylulose but not of xylose in *Saccharomyces cerevisiae* TMB3001. *FEMS Yeast Res* **2**: 277–282.

Kanagasundaram V, Scopes RK. 1992. Cloning, sequence analysis, and expression of the structural gene encoding glucose-fructose oxidoreductase from *Zymomonas mobilis*. *J Bacteriol* **174**: 1439–1447.

Kötter P, Amore R, Hollenberg CP, Ciriacy M. 1990. Isolation and characterization of the *Pichia stipitis* xylitol dehydrogenase gene, XYL2, and construction of a xylose-utilizing *Saccharomyces cerevisiae* transformant. *Curr Genet* **18**: 493–500.

Kötter P, Ciriacy M. 1993. Xylose fermentation by *Saccharomyces cerevisiae*. *Appl Microbiol Biotechnol* **38**: 776–783.

Kuhn A, van Zyl C, van Tonder A, Prior BA. 1995. Purification and partial characterization of an aldo-keto reductase from *Saccharomyces cerevisiae*. *Appl Environm Microbiol* **61**: 1580–1585.

Laemmli UK. 1970. Cleavage of structural proteins during the assembly of the head of bacteriophage T_4. *Nature* **227**: 680–685.

Larsson C, Påhlman IL, Ansell R, *et al*. 1998. The importance of the glycerol 3-phosphate shuttle during aerobic growth of *Saccharomyces cerevisiae*. *Yeast* **14**: 347–357.

Lodi T, Guiard B. 1991. Complex transcriptional regulation of the *Saccharomyces cerevisiae CYB2* gene encoding cytochrome b_2: CYP1(HAP1) activator binds to the *CYB2* upstream activation site UAS1-B2. *Mol Cell Biol* **11**: 3762–3772.

Meijer MM, Boonstra J, Verkleij AJ, Verrips CT. 1998. Glucose repression in *Saccharomyces cerevisiae* is related to the glucose concentration rather than the glucose flux. *J Biol Chem* **273**: 24 102–24 107.

Meinander NQ, Hahn-Hägerdal B. 1997. Influence of co-substrate concentration on xylose conversion by recombinant, *XYL1*-expressing *Saccharomyces cerevisiae*: a comparison of different sugars and ethanol as co-substrates. *Appl Environm Microbiol* **63**: 1959–1964.

Mellor J, Dobson MJ, Roberts NA, *et al*. 1983. Efficient synthesis of enzymatically active calf chymosin in *Saccharomyces cerevisiae*. *Gene* **24**: 1–14.

Müller S, Boles E, May M, Zimmermann FK. 1995. Different internal metabolites trigger the induction of glycolytic gene expression in *Saccharomyces cerevisiae*. *J Bacteriol* **177**: 4517–4519.

Norbeck J, Blomberg A. 1997. Metabolic and regulatory changes associated with growth of *Saccharomyces cerevisiae* in 1.4 M NaCl. Evidence for osmotic induction of glycerol dissimilation via the dihydroxyacetone pathway. *J Biol Chem* **272**: 5544–5554.

O'Connell KL, Stults JT. 1997. Identification of mouse liver proteins on two-dimensional electrophoresis gels by matrix-assisted laser desorption/ionization mass spectrometry of *in situ* enzymatic digests. *Electrophoresis* **18**: 349–359.

Påhlman AK, Granath K, Ansell R, Hohmann S, Adler L. 2001. The yeast glycerol 3-phosphatases Gpp1p and Gpp2p are required for glycerol biosynthesis and differentially involved in the cellular responses to osmotic, anaerobic, and oxidative stress. *J Biol Chem* **276**: 3555–3563.

Perrot M, Sagliocco F, Mini T, *et al*. 1999. Two-dimensional gel protein database of *Saccharomyces cerevisiae* (update 1999). *Electrophoresis* **20**: 2280–2298.

Pitkänen J-P, Aristidou A, Salusjärvi L, Ruohonen L, Penttilä M. 2002. Metabolic flux analysis of xylose metabolism in recombinant *Saccharomyces cerevisiae* using continuous culture. *Metab Eng* (in press).

Poutanen M, Salusjärvi L, Ruohonen L, Penttilä M, Kalkkinen N. 2001. Use of matrix-assisted laser desorption/ionization time-of-flight mass mapping and nanospray liquid chromatography/electrospray ionization tandem mass spectrometry sequence tag analysis for high sensitivity identification of yeast proteins separated by two-dimensional gel electrophoresis. *Rapid Comm Mass Spectrom* **15**: 1685–1692.

Ramil E, Agrimonti C, Shechter E, Gervais M, Guiard B. 2000. Regulation of the *CYB2* gene expression: transcriptional coordination by the Hap1p, Hap2/3/4/5p and Adr1p transcription factors. *Mol Microbiol* **37**: 1116–1132.

Remize F, Andrieu E, Dequin S. 2000. Engineering of the pyruvate dehydrogenase bypass in *Saccharomyces cerevisiae*: role of the cytosolic $Mg(^{2+})$ and mitochondrial $K(^{+})$ acetaldehyde dehydrogenases Ald6p and Ald4p in acetate formation during alcoholic fermentation. *Appl Environm Microbiol* **66**: 3151–3159.

Richard P, Toivari MH, Penttilä M. 1999. Evidence that the gene YLR070c of *Saccharomyces cerevisiae* encodes a xylitol dehydrogenase. *FEBS Lett* **457**: 135–138.

Richard P, Toivari MH, Penttilä M. 2000. The role of xylulokinase in *Saccharomyces cerevisiae* xylulose catabolism. *FEMS Microbiol Lett* **190**: 39–43.

Ruohonen L, Aalto MK, Keränen S. 1995. Modifications to the *ADH1* promoter of *Saccharomyces cerevisiae* for efficient production of heterologous proteins. *J Biotechnol* **39**: 193.

Shevchenko A, Jensen ON, Podtelejnikov AV, *et al*. 1996. Linking genome and proteome by mass spectrometry: large-scale identification of yeast proteins from two-dimensional gels. *Proc Natl Acad Sci USA* **93**: 14 440–14 445.

Sierkstra LN, Verbakel JM, Verrips CT. 1992. Analysis of transcription and translation of glycolytic enzymes in glucose-limited continuous cultures of *Saccharomyces cerevisiae*. *J Gen Microbiol* **138**(12): 2559–2566.

ter Linde JJ, Liang H, Davis RW, *et al*. 1999. Genome-wide transcriptional analysis of aerobic and anaerobic chemostat cultures of *Saccharomyces cerevisiae*. *J Bacteriol* **181**: 7409–7413.

Toivari MH, Aristidou A, Ruohonen L, Penttilä M. 2001. Conversion of xylose to ethanol by recombinant *Saccharomyces cerevisiae*: importance of xylulokinase (XKS1) and oxygen availability. *Metab Eng* **3**: 236–249.

Uetz P, Giot L, Cagney G, *et al*. 2000. A comprehensive analysis of protein–protein interactions in *Saccharomyces cerevisiae*. *Nature* **403**: 623–627.

van Zyl C, Prior BA, Kilian SG, Kock JL. 1989. D-xylose utilization by *Saccharomyces cerevisiae*. *J Gen Microbiol* **135**: 2791–2798.

Vido K, Spector D, Lagniel G, Lopez S, Toledano MB, Labarre J. 2001. A proteome analysis of the cadmium response in *Saccharomyces cerevisiae*. *J Biol Chem* **276**: 8469–8474.

Walfridsson M, Hallborn J, Penttilä M, Keränen S, Hahn-Hägerdal B. 1995. Xylose-metabolizing *Saccharomyces cerevisiae* strains overexpressing the *TKL1* and *TAL1* genes encoding the pentose phosphate pathway enzymes transketolase and transaldolase. *Appl Environm Microbiol* **61**: 4184–4190.

Wahlbom CF, Eliasson A, Hahn-Hägerdal B. 2001. Intracellular fluxes in a recombinant xylose-utilizing *Saccharomyces cerevisiae* cultivated anaerobically at different dilution rates and feed concentrations. *Biotechnol Bioeng* **72**: 289–296.

Wang X, Mann CJ, Bai Y, Ni L, Weiner H. 1998. Molecular cloning, characterization, and potential roles of cytosolic and mitochondrial aldehyde dehydrogenases in ethanol metabolism in *Saccharomyces cerevisiae*. *J Bacteriol* **180**: 822–830.

Zachariou M, Scopes RK. 1986. Glucose-fructose oxidoreductase, a new enzyme isolated from *Zymomonas mobilis* that is responsible for sorbitol production. *J Bacteriol* **167**: 863–869.

